The role of memory network topology in predicting the effect of exogenous brain stimulation

Simon W. Davis[1, 2, 3], Bruce Luber[2], David L.K. Murphy[2],

Sarah H. Lisanby[2], and Roberto Cabeza[1]

[1]Center for Cognitive Neuroscience, Duke University, 27708; [2]Division of Brain Stimulation, Department of Psychiatry and Behavioral Sciences, Duke University School of Medicine, 27708; [3]Department of Neurology, Duke University School of Medicine, 27708.

Abbreviated title: Causal Network Dynamics in Aging

Corresponding author: Simon W Davis
Department of Neurology
Box 2900, DUMC, Duke University
Durham, NC 27708
simon.davis@duke.edu

Pages: 34; Tables: 1; Figures: 8
Words: Abstract: 200; Introduction: 647; Discussion: 1455.
COI: No COI.

Acknowledgements: This work was supported by National Institutes of Health Grant R01 AG19731.

Abstract (141/150 words)

Lesion and functional neuroimaging evidence suggest that local network deficits can be compensated by global network over-recruitment during a cognitive task. However, the neural mechanisms linking local and global network changes remain uncertain. To investigate this issue, we manipulated local function using repetitive transcranial magnetic stimulation (rTMS) and measured structural and task-based functional network organization during memory encoding. The study yielded two main findings. First, consistent with the compensation hypothesis, 1-Hz rTMS attenuated local activity in the stimulated left prefrontal cortex (PFC) but increased the connectivity of this region with other brain areas, including contralateral PFC. Second, this 1-Hz-related increase in global connectivity effects was associated with the volume of more global connections, suggesting white-matter constraints adaptive changes in functional connectivity. Taken together, these results clarify the neural mechanisms linking local and global network changes and the role of structural connectivity.

Introduction

Over the past few decades, transcranial magnetic stimulation (TMS) has developed into a powerful tool to establish causal brain-behavior relationships (Hanslmayr et al., 2014; Luber and Lisanby, 2014). TMS has *local effects* in the cortical region stimulated, as well as *global effects* in other regions of the network (Nahas et al., 2001; Hoogendam et al., 2010). Studies combining TMS with fMRI or EEG have shown that TMS effects spread through white-matter connections to distant brain regions (Bestmann et al., 2004; Wang et al., 2014). However, the neural mechanisms linking local and global TMS effects remain uncertain. We investigated this question by combining repetitive TMS (rTMS) with activity and functional connectivity measures provided by functional MRI (fMRI) and with white-matter integrity measures supplied by diffusion tensor imaging (DTI).

The current study had two main goals. The first goal was to investigate the impact of TMS-related local dysfunction on global brain function. Computational models have shown that neural networks are relatively resistant to local damage because processing demands are often shifted from impaired nodes to intact nodes (Fornito et al., 2015). In other words, *local dysfunction* can be compensated by *global over-recruitment*. Consistent with this *compensation hypothesis*, there is abundant neuropsychological evidence that focal brain damage can be partially counteracted by the over-recruitment of spared brain regions (Seeley et al., 2009). For example, the recovery of motor (Zemke et al., 2003) or language (Saur et al., 2010) functions following damage of critical regions in one hemisphere has been associated with over-recruitment of regions in the unaffected hemisphere. TMS provides a method to investigate the link between local dysfunction and global over-recruitment in healthy humans.

We investigated link between local vs. global function by combining rTMS with fMRI-based functional connectivity measures, quantified using graph-based *modularity* analyses (Chang et al., 2012). Modularity refers to a network architecture where groups of nodes communicate more intimately with each other than with other nodes in the network. A modular network requires both *within-module* connectivity or *degree* (WMD) and *between-module* connectivity or *degree* (BMD). In general, lower TMS frequencies (e.g., 1-Hz) tend to reduce brain activity in the stimulated region (de Vries et al., 2012) whereas higher rTMS frequencies (>5 Hz) tend to increase it (Schneider et al., 2010). Thus, we predicted that *1-Hz rTMS would reduce activity in the stimulated region (local activity) but increase its BMD (global connectivity)—consistent with the compensation hypothesis, whereas 5-Hz rTMS would increase both activity and WMD in the stimulated region (Prediction 1).*

Our second goal was to relate the effects of rTMS on WMD and BMD to integrity of white-matter tracts connecting the stimulated region to the rest of the network. There is abundant evidence that functional connectivity depends on quality of white-matter tracts connecting different regions (Gong et al., 2009; Horn et al., 2014). Thus, it follows that global TMS effects should be moderated by integrity of white-matter tracts. Assuming that our first prediction would be confirmed and 1-Hz rTMS, but not 5-Hz rTMS, would increase BMD, we expected white-matter to moderate functional connectivity specifically in the 1-Hz condition. Thus, we predicted that *the global connectivity of the stimulated region should be correlated with white-matter integrity in the 1-Hz but not the 5-Hz rTMS condition* (*Prediction 2*).

We chose to investigate our two predictions in older adults for two main reasons. First, older adults are an ideal group to test the prediction that local dysfunction is

compensated by global over-recruitment. There is abundant functional neuroimaging evidence that, consistent with the compensation hypothesis, older adults show weaker activity than younger adults in the main components of the task network but over-recruitment of distant regions of the network (Cabeza, 2002; Spreng et al., 2010). These changes have been found not only for brain activity but also for functional connectivity, with evidence that older adults show stronger long-range functionally connectivity than younger adults outside of local cortical communities (Dennis et al., 2008; Spaniol and Grady, 2012; Geerligs et al., 2015). Second, older adults are an ideal group to investigate how functional connectivity is modulated by white-matter integrity. To link functional connectivity and white-matter it is critical to investigate a group with substantial individual differences in white-matter integrity and older adults display show them. Also, we have previously demonstrated in older adults that functional connectivity between specific pairs of brain regions is significantly correlated with DTI measures of white-matter tracts connecting them (Davis et al., 2012; Daselaar et al., 2014).

In sum, we investigated in older adults (1) the relationship between local and global rTMS effects, and (2) the link between global rTMS effects and white-matter integrity. Because we used rTMS as a physiological probe (Clapp et al., 2010; Feredoes et al., 2011) and the rTMS dosing was constrained by MRI scanning context, we did not expect significant behavioral effects on the scanned memory task. Instead, we focused on the physiological effects of rTMS on memory-related activity and functional connectivity, as measured by the difference between subsequently remembered vs. forgotten trials or *subsequent memory effect*—SME (Paller and Wagner, 2002). Thus, we investigated differential effects of 1-Hz and 5-Hz rTMS on the SME and then relate them to white-matter measures.

Methods

Participants

Fourteen healthy older adults were originally recruited for the study (all native English speakers; 7 females; age mean +/- SD, 66.7 +/- 3.9 years; range 61-74 years), but subject who did not tolerate rTMS was removed from the analyses. Each older adult was screened for exclusion criteria for TMS (history of seizure, brain/head injuries) as well as psychiatric condition (MINI International Neuropsychiatric Interview, English Version 5.0.0 DSM-IV, Sheehan et al., 2006). None of the older participants reported subjective memory complaints in everyday life or had MMSE score below 27 (mean +/- SD = 29.1 +/- 0.8).

Procedures

Study structure and TMS setup

The study consisted of two sessions, 1-4 days apart (see **Figure 1**). During Session 1, participants were fMRI-scanned during a sentence learning task, and brain activity associated with successful encoding was identified by comparing activity for subsequently remembered vs. forgotten sentences (*subsequent memory effect*—SME). The region showing the largest SME within the *left middle frontal gyrus* (LMFG) was identified as the TMS target. In addition of identifying the TMS target, fMRI activity during Session 1 provided a TMS-independent baseline level of SME. During Session 2, the subject-specific LMFG target was stimulated with 1-Hz and 5-Hz rTMS (order counterbalanced) and the effects on functional connectivity were immediately measured with fMRI. Session 2 also included a block in which single-pulse TMS was delivered during fMRI (concurrent TMS-fMRI).

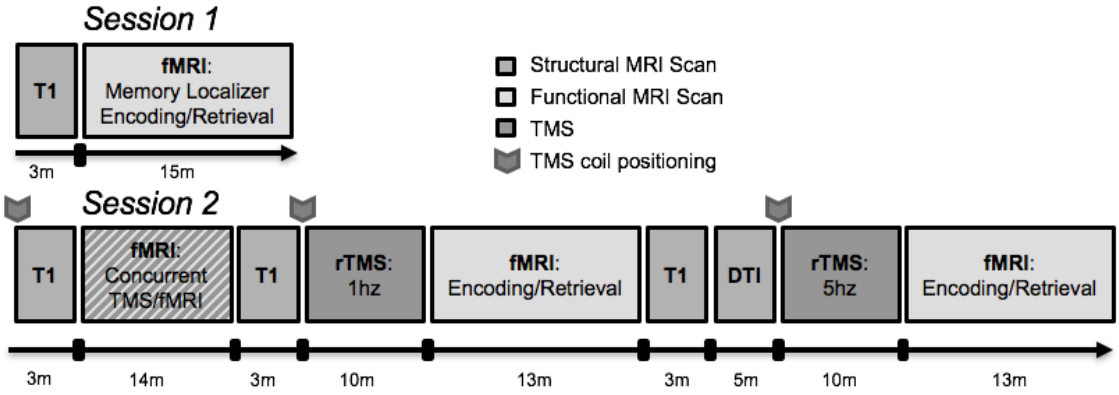

Figure 1. Data acquisition schedule.

Between Session 1 and 2, fMRI data from Session 1 was used to identify the LMFG region showing the greatest difference in activity between subsequently remembered vs. forgotten sentences. At the beginning of Session 2, co-registered fMRI and structural MRI images were used to identify using Brainsight (Rogue Research, Montreal) the ideal scalp location for stimulating the LMFG target, which was marked in a tight-fitting swim cap. After acclimating each participant to TMS at different frequencies, the motor threshold (MT) was determined using MagVenture R30M (MRI-compatible TMS system). MTs were determined using electromyography of the right first dorsal interosseous (FDI) muscle and defined as the lowest setting of TMS device intensity at which ≥ 5 out of 10 motor evoked potentials of at least 50μV peak to peak amplitude could be elicited.

Task-based fMRI preceded by rTMS

After the two concurrent TMS-fMRI runs, participants underwent two fMRI runs in which they performed the same sentence learning task used to identify the subject-specific LMFG target in Session 1. In each run, participants encoded 60 sentences (e.g., "A SURFBOARD was on top of the TRUCK.") trying to imagine the situation described in each sentence, and then performed an associative recognition test in which

they distinguished between identical (e.g., surfboard-truck) and recombined (e.g., surfboard-table) word-pairs.

Coplanar functional images were acquired with an 8-channel head coil using an inverse spiral sequence with the following imaging parameters: flip angle = 77°, TR = 2000ms, TE = 31ms, FOV = 24.0 mm^2, and a slice thickness of 3.8mm, for 37 slices. The position of the TMS coil was reset to the same target site before the beginning of each rTMS session, and monitored continuously during the run.

Critically, each task-based fMRI run was preceded by 10 minutes of rTMS at 120% MT. rTMS did not have a significant effect on memory performance, which is not reported. Before one run, 1-Hz rTMS was delivered in a continuous train, and before the other run, 5-Hz rTMS was delivered in intermittent 6 sec trains with a 24 sec inter-train interval. Thus, dosage was equivalent between 1Hz and 5Hz rTMS conditions (600 total pulses). The order of the two frequency conditions was counterbalanced across participants.

Data Analyses

The general analytical pipeline is depicted in **Figure 2**. Briefly, both functional and structural imaging data were processed according to standard preprocessing heuristics (see below), and adjacency matrices comprising psychophysiological interaction (PPI)-based functional correlations associated with the task (fMRI data) or structural connections based on tractography streamline counts (DWI data) were evaluated. Modularity was based solely on structural connectivity, and regions within a high-dimensional atlas (n = 471 regions) were partitioned using conditional expected models (Chang et al., 2012). In order to compare functional and structural networks we use graph-theoretical methods to find the distance traversed by the lowest weighted path

in a structural network, which is constructed by connecting each cortical region with a weighted edge. We proceed stepwise, by relating our functional network $\boldsymbol{A_{fMRI}}$ to our structural network $\boldsymbol{A_{DTI}}$, at structural paths of length $\boldsymbol{l}$, by which we are able to demonstrate the value of both local (direct) and long-distance (indirect) paths in promoting success-related connectivity.

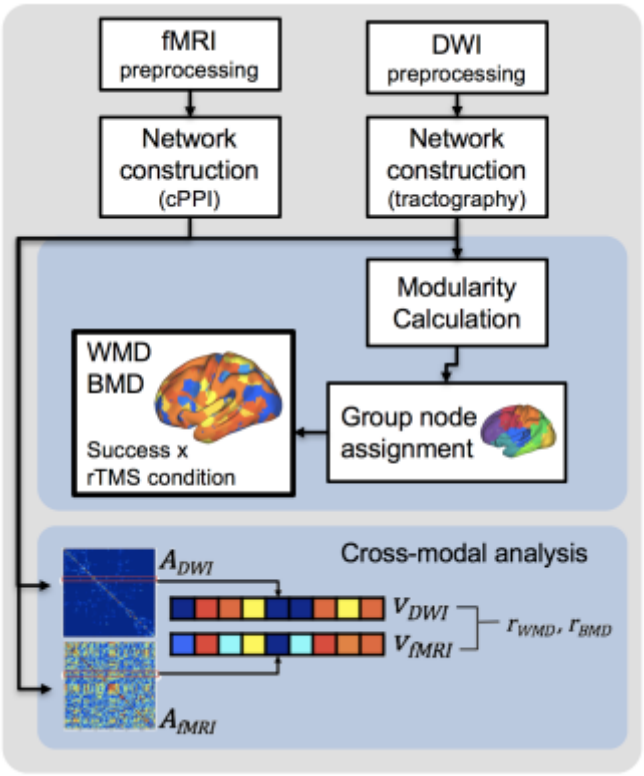

Figure 2. Analytical pipeline.

Structural and functional preprocessing

Diffusion-weighted images were preprocessed using typical methods, including brain extraction, correction for eddy-current distortion and simple head motion, and correction of the b-matrix for any rigid-body coregistration completed in this step (Smith et al., 2006). Fractional anisotropy (FA) images were generated using the tensor model from *dtifit* (FSL, www.fmrib.ox.ac.uk/fsl/). The preprocessing of functional data for both

the localizer, and post-rTMS conditions was carried out using image processing tools from FSL 5.01 (FMRIB, Oxford, UK). Images were corrected for slice acquisition timing, motion, and linear trend; temporally smoothed with a high-pass filter using a 190s cutoff; and normalized to the Montreal Neurological Institute (MNI) stereotaxic space. Spatial filtering with a Gaussian kernel of full-width half-maximum (FWHM) of 6mm was applied. Voxel time-series analysis was carried out using general linear modeling (GLM); fixed effects models were carried out to examine the effects of 1) both memory success and stimulation frequency in the localizer and post-rTMS data. We modeled encoding trials that were either subsequently remembered or subsequently forgotten, in order to examine standard subsequent memory effects (SMEs) in the localizer, post-1Hz rTMS, and post-5Hz rTMS runs.

Construction of connectivity matrices

Before either structural or functional matrices were constructed, we first sought to establish a consistent parcellation scheme across all image types that reflects an accurate summary of full connectome effects (Bellec et al., 2015). Subjects' T1-weighted images were segmented using the SPM12 (www.fil.ion.ucl.ac.uk/spm/software/spm12/), yielding a grey matter (GM) and white matter (WM) mask in the T1 native space for each subject. The entire GM was then parcellated into 471 regions of interest (ROIs), each representing a network node by using a subparcellated version of the Harvard-Oxford Atlas, (Tzourio-Mazoyer et al., 2002), defined originally in MNI space. The T1-weighted image was then nonlinearly normalized to the ICBM152 template in MNI space using fMRIB's Non-linear Image Registration Tool (FNIRT, FSL, www.fmrib.ox.ac.uk/fsl/). The inverse transformations were applied to the HOA atlas in the MNI space, resulting in native-T1-space GM parcellations for each subject. Then, T1-weigted images were coregistered to native diffusion space using the subjects' unweighted diffusion image as

a target; this transformation matrix was then applied to the GM parcellations above, resulting in a native-diffusion-space parcellation for each subject.

For structural connection matrices, network edges were defined by the number of tractography streamlines between any two ROIs. We used Dipy (Garyfallidis et al., 2014) to fit the data with the constant solid angle (CSA) model with fourth-order spherical harmonics, and generating generalized FA (GFA) maps from estimated orientation distribution functions. Using a deterministic tracking algorithm (EuDX; Garyfallidis et al., 2012) with standard tracking parameters (step size: 0.5mm, turning angle 45°, alpha = 0.05). Whole-brain streamlines (~30,000 per subject) were saved for subsequent parcellation into structural connectivity matrices (see below). Streamlines were filtered out if the two terminal points were located in the two node regions. Because a larger region is more likely to generate a larger number of streamlines, this fiber-density weighted network (Zhong et al., 2015) was corrected for nodal size $M_{i,j} = (2 \times FN)/(n_i + n_j)$, where n_i and n_j denote the number of voxels in regions *i* and *j*, respectively, and FN denotes the fiber number linking region *i* and region *j* (Cheng et al., 2012). Lastly, we corrected for spurious node pairs using a correction method described previously (Gong et al., 2009).

Functional connection matrices representing task-related connection strengths were estimated using a correlational psychophysical interaction (cPPI) analysis (Fornito et al., 2011). Briefly, the model relies on the calculation of a PPI regressor for each region, based on the product of that region's timecourse and a task regressor of interest, in order to generate a term reflecting the psychophysical interaction between the seed region's activity and the specified experimental manipulation. In the current study the task regressors based on the convolved task regressors from the univariate model

described above were used as the psychological regressor, which coded subsequently remembered and subsequently forgotten word pairs with positive and negative weights, respectively, of equal value. This psychological regressor was multiplied with two network timecourses for region i and j. We then computed the partial correlation $\rho_{PPI_i,PPI_j \cdot z}$, removing the variance z associated with the psychological regressor, the timecourses for regions i and j, and constituent noise regressors. We accounted for the potential effects of head motion and other confounds by assessing the 6 motion parameters and including these parameters in our partial correlation between regions.

Graph Theory Metrics

The graph theoretic approach used in the current manuscript focuses on two key mechanistic concepts: modularity and degree. Degree is a basic graph-theoretic measure describing the sum of edges at a node i in weighted networks, while modularity is a measure originally derived for quantifying the quality of a partition (Newman and Girvan, 2004). Fundamental to the definition of modularity is the computation of a proper null network, i.e. a null network, R, with the same number of nodes and node degrees but otherwise no underlying structure. If a natural division of a network exists, we should expect within-module connections between node i and j (A_{ij}) to be stronger than a random network R_{ij}, and connections between modules should be weaker than the same random network. Thus, modularity is higher the more partitioned a network is into modules that are densely connected within rather than between themselves. For a given partition of nodes of a network into modules, the modularity Q of this partition is

Eqn. 1.

$$Q = \frac{1}{2m}\sum_{i,j}\left(A_{ij} - R_{ij}\right)\delta(C_i, C_j)$$

where m C_i indicates group membership of node i. Therefore, modularity increases when $A_{ij} - R_{ij}$ (edge strength minus expected edge strength) is positive for within-module edges. Standard modularity analysis defines the null distribution (i.e., R_{ij}) from a randomization of the rows of the input matrix (Newman, 2006). However, even random networks can exhibit high modularity because of incidental concentrations of edges. This method of computing the null is also problematic for our analysis because it ignores negative connection weights and implicitly assumes self-loops (connections from nodes to themselves), which are meaningless in the functional networks considered here. Furthermore, modularity partitions based on randomized null distributions suffer from inconsistency in partition assignments over repeated executions of the same algorithm, and rely instead on permuting the algorithm for the maximum Q. We therefore employ a more recently developed modularity algorithm (Chang et al., 2014) that relies on a transformed Tracy-Widom distribution in order to more adequately model the null distribution in a modularity computation, linking standard module detection with random matrix theory.

Generally, the sum, of edges, or connections between a node and other nodes in the network, defines the node's degree. We examined whether the distribution of node degree values, either within or between a set of cortical modules, differed between successful and unsuccessfully encoded trials, following previous studies focusing on degree (Guimera and Nunes Amaral, 2005). Critically, we considered changes in degree distribution at each node either with respect to its surrounding module (within-module degree or WMD), or as a function of a node's relationship with more distant cortical modules (between-module degree or BMD). Both WMD and BMD use the same underlying function to estimate degree:

Eqn. 2

$$z_i = \frac{\kappa_i - \kappa_{S_i}}{\sigma_{K_{S_i}}}$$

where κ_{S_i} is the average of K over all the nodes in S_i, and $\sigma_{K_{S_i}}$ is the standard deviation of κ. in S_i. This within-module degree z-score ($z_{i_{WMD}}$) measures how well connected node i is to other nodes within the module, while the between-module degree z-score ($z_{i_{BMD_m}}$) measures how well connected a node i is to other nodes with another module M in the cortical parcellation. As such, the calculation of $z_{i_{BMD}}$ is repeated for each pair of modules. In typical applications, nodes with a high z_{WMD} are interpreted to represent local, intramodular information-processing hubs, whereas nodes with high z_{BMD} show a relatively even distribution of connectivity across all modules (Fornito et al., 2012).

Cross-modal comparisons

Lastly, we sought to test the hypothesis that the regions that are most affected by rTMS stimulation are best predicted by the structural connectivity with the stimulation site. A number of recent analyses have focused on first-order correlations between a structural connectivity matrix $\boldsymbol{A_{DTI}}$ and a functional connectivity matrix $\boldsymbol{A_{fMRI}}$, for a given region *R*, based on the assumption that direct structural connectivity should engender a corresponding modulation of functional connectivity (Zimmermann et al., 2016). The agreement of functional and structural connectivity between all regions was therefore calculated using a novel method of estimating the functional-structural relationship as a function of the structural path length in a structural matrix $\boldsymbol{A_{DTI}}$.

We then calculated the Pearson's product moment correlation between a vector describing the structural connectivity for both within-module connections ($v_{DWI_{WMD}}$) and

between module connections ($v_{DWI_{BMD}}$), and vectors describing the corresponding vectors for functional connectivity v_{fMRI}; given the role of negative correlations described above, we used the absolute value of the functional connectivity information for each condition. This cross-modal correlation was then repeated for both 1Hz and 5Hz functional matrices, using only the vector describing connectivity from the site of stimulation (as quantified by in-scanner fiducial markers). Statistical significance in both global and region-specific relationships were obtained by Fisher-transforming the *r*-values obtained for each subject and calculating paired-sample t-tests between 1Hz and 5Hz conditions; WMD and BMD were not compared directly, as these measures represent distinct distributions of connectivity values, with different numbers of contributing connections, and are thus not directly comparable conditions.

Results

As explained in the Introduction, our goals were to investigate (1) the effects of TMS on local activity and global connectivity, and (2) how these effects are modulated by white-matter integrity. Consistent with our intended use of TMS as a physiological probe (Clapp et al., 2010; Feredoes et al., 2011), memory performance did not differ between rTMS conditions (d' was 2.35 and 2.46 in the 1-Hz and 5-Hz rTMS conditions, respectively; $t_{13} = 0.65$, $p = 0.6$), nor did reaction times to correct trials ($t13 = 1.14$, $p = 0.3$). As expected, however, rTMS did significantly modulate memory-related activity and functional connectivity, as isolated by the subsequently remembered vs. forgotten contrast (subsequent memory effect—SME). Analyses on the effects of TMS and links to DTI measures focus on memory-related activity and connectivity (SMEs).

Effects of TMS on memory-related activity and connectivity

Our first prediction was that *1-Hz rTMS would reduce activity in the stimulated region (local activity) but increase its BMD (global connectivity)—consistent with the compensation hypothesis, whereas 5-Hz rTMS would increase both activity and WMD in the stimulated region.* We first investigated the effects of rTMS on activity in the stimulated brain region (LMFG) and then turned to rTMS effects on BMD and WMD.

rTMS effects on memory-related activity. Before focusing on the stimulated region, we performed a whole-brain analysis, whose results are displayed in **Figure 3**. Compared to a localizer (no rTMS) condition, 1-Hz rTMS reduced SMEs in several brain regions, whereas 5-Hz rTMS enhanced SMEs in multiple areas. Critically, consistent with our first prediction, the SME in the stimulated LMFG region, shown in red in **Figure 3B**, was reduced by 1-Hz rTMS but increased by 5-Hz rTMS; pairwise comparisons between 1Hz and 5Hz activity for successfully remembered trials was highly significant ($t_{13} = 3.43$, $p < 0.001$). Having confirmed that rTMS modulated memory-related activity, we then turned to the effects of rTMS on BMD and WMD.

.

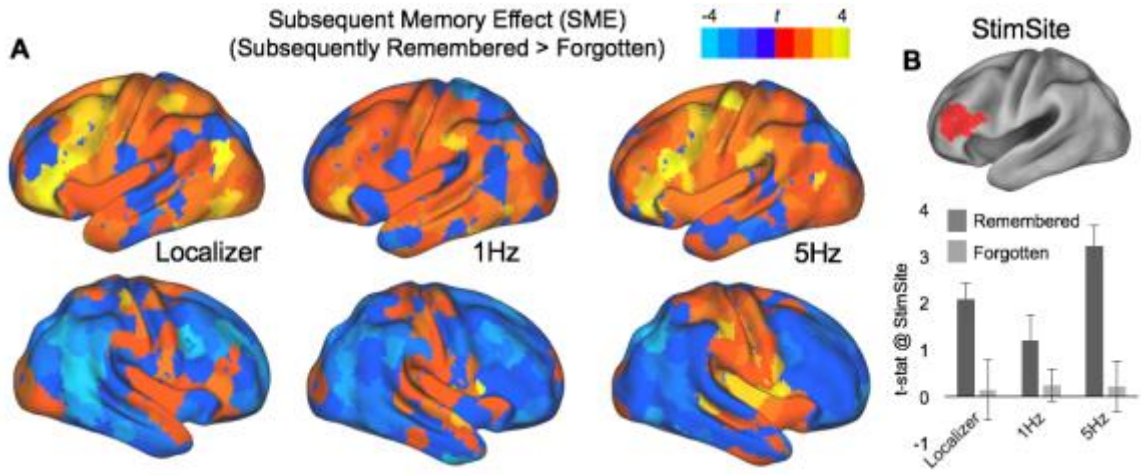

Figure 3. Effects of rTMS on subsequent memory effects (SMEs=remember-forgotten). (**A**) Effects on 471 cortical ROIs, during Localizer memory test. (**B**) The left PFC Stimulation Site within LMFG is shown in red, with standard effects for subsequently Remembered and Forgotten trials during Localizer, 1Hz, and 5Hz. rTMS conditions within this ROI.

Effects of rTMS on between-module degree (BMD). The modularity analysis based on diffusion tractography connectivity (adjusted streamlines) strong modularity (Q = 0.71 across 100 permutations), with 16 distinct, symmetrical communities formed from the averaged structural connectome in our sample; community assignments are depicted in **Figure 4**. Each module comprises between 68 and 120 individual nodes. Within-module degree (WMD) quantifies functional connectivity among the nodes within each module, whereas between-module degree (BMD) assesses functional connectivity between different modules. We first considered the effects of rTMS on between-module degree (BMD).

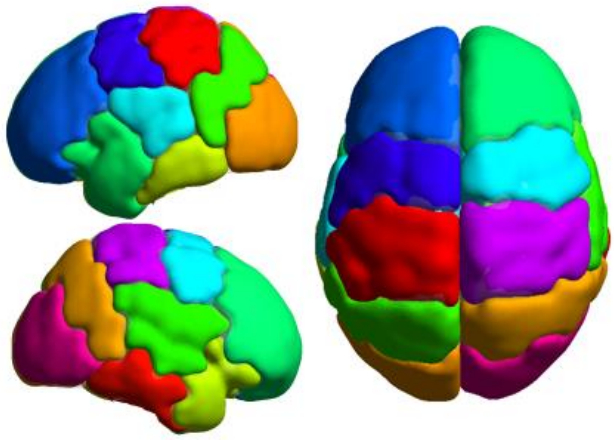

Figure 4. Structural module assignment.

On the basis of the compensation hypothesis, we predicted that a 1-Hz rTMS condition that reduced local activity, which we confirmed, would tend to increase BMD. Consistent with this prediction, the 1-Hz rTMS yielded large memory-related BMD increases in bilateral PFC regions. In contrast with 1-Hz rTMS, 5-Hz rTMS produced limited effects in two small regions, the left anterior superior temporal gyrus ($t_{12} = 3.15$, $p < 0.01$) and right Heschel's gyrus ($t_{12} = 3.45$, $p < 0.01$).

To clarify the source of BMD increases in left PFC in the 1-Hz rTMS condition, we calculated the proportion of BMD connections from left PFC to other modules, which are shown in **Figure 5**. Although parietal regions make important contributions, the BMD increase in left PFC was primarily driven by its connections with right PFC, which accounted for 49% of all significant BMD connections and also showed a memory-related BMD increases (**Figure 6**). Post-hoc tests indicated that the WMD increases in left PFC were significantly due to enhanced connectivity with right MFG (mean z_{BMD} to right PFC module = 3.35; to all other modules < 1.0). It is worth noting that although right MFG was not directly stimulated with rTMS, it has strong white-matter connections with the stimulated LMFG ROI, which can explain the BMD effects. In sum, consistent with

our first prediction, 1-Hz rTMS on LMFG reduced its activity but enhanced its connectivity with the rest of the brain, and particularly with contralateral right PFC regions. These findings provide direct support to the compensation hypothesis.

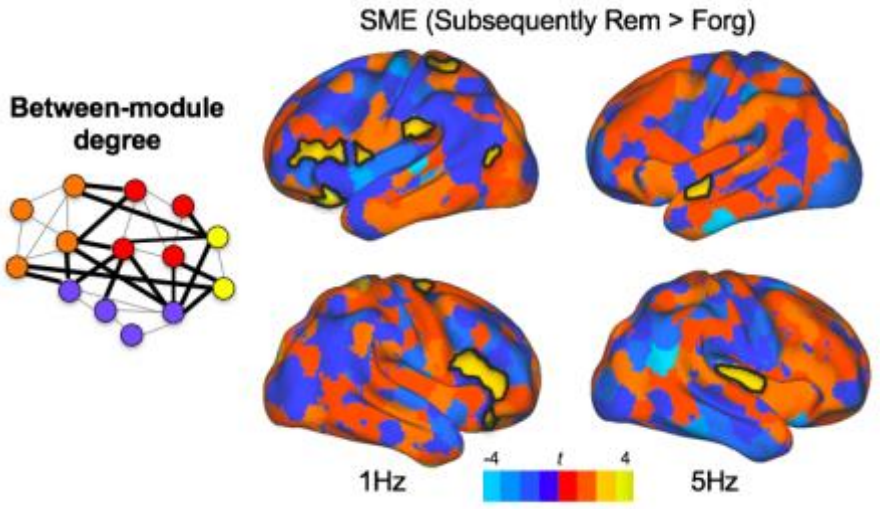

Figure 5. Between-Module Degree (BMD) associated with SME across rTMS conditions. Regions showing significant rTMS effects are outlined in black.

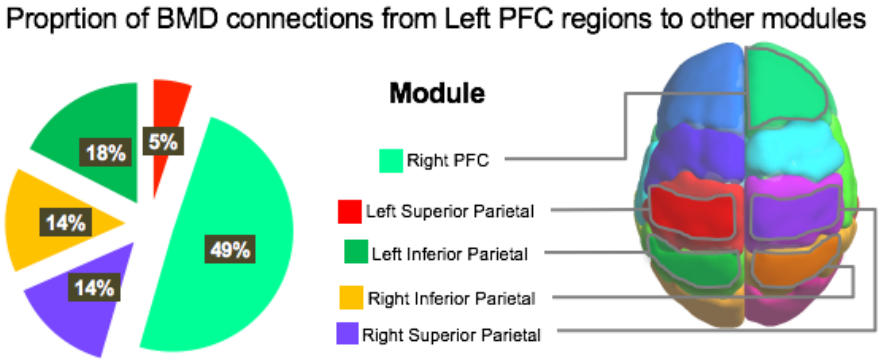

Figure 6. Between module connections in the 1Hz condition are largely attributable to a higher proportion of connectivity to contralateral Right PFC module (which also shows a success-related increase in BMD See **Figure 5**).

To more directly test the compensation hypothesis, we investigated if the extent to which 1-Hz rTMS reduced activity in LMFG correlated with the extent to which it increased the BMD of this region. As illustrated by **Figure 7**, we found a reliable negative correlation across subjects (r_{12} = -0.21), across all left PFC nodes, between univariate fMRI activity and BMD during remembered trials but not during forgotten trials. This effect was selective for the 1-Hz rTMS condition, during which the local SME in fMRI univariate activity was attenuated (see **Figure 3**), and was not present in the 5-Hz rTMS condition, which had the opposite effect on local fMRI activity. No such relationships were observed in the relationship between univariate activity and WMD (all $r < 0.05$). Thus, there more 1-Hz rTMS impaired memory-related left PFC functions the more it increased its memory-related connections with the rest of the brain, a result clearly consistent with the compensation hypothesis.

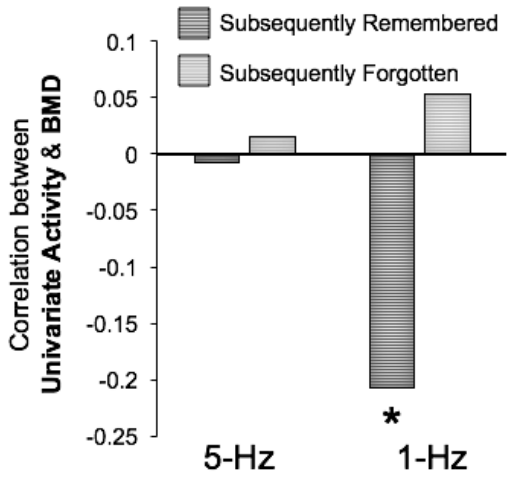

Figure 7. Relationship (Pearson's r) between left PFC univariate activity for Subsequently Remembered and Subsequently Forgotten trials during encoding and distant connectivity (BMD) between the left PFC module and all other modules. Because BMD characterizes more long range connections.

Lastly, we sought validate this relationship by testing the alternative hypothesis that task-related increases in distant connectivity reflects merely a nonselective response associated with age-related declines in brain health, and could be elicited by a stimulation train in absence of a cognitive task. Regional stimulation-related increases in univariate activity were observed in left DLPFC/IFG, as well as left temporal cortex. Critically, task-related BMD increases observed above after 1Hz stimulation were unrelated to BMD at the same site of stimulation (r = -0.08, **Figure 8**).

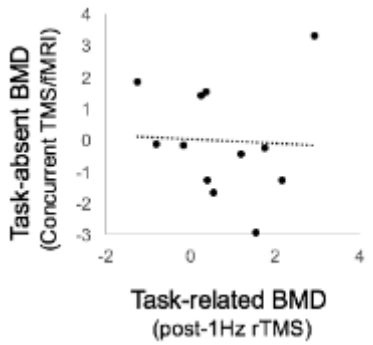

Figure 8. Concurrent TMS/fMRI. Critically, task-related BMD increases observed above after 1Hz stimulation were unrelated to BMD at the same site of stimulation (r = -0.08).

Effects of rTMS on within-module degree (WMD). The second part of our first prediction is that a 5-Hz rTMS condition that enhances activity in the stimulated region would lead to a WMD increase in this region. Consistent with this prediction, **Figure 9** clearly shows that WMD in the stimulated LMFG region was enhanced by 5-Hz rTMS but not in the 1-Hz rTMS ($t_{12} = 2.28$, $p < 0.05$). Additionally, 5-Hz rTMS also increased memory-related WMD in right PFC ($t_{12} = 2.12$, $p < 0.05$), the left angular gyrus ($t_{12} = 2.78$, $p < 0.01$) and the right hippocampus ($t_{12} = 2.36$, $p < 0.01$). In contrast, 1-Hz yielded only minor WMD increases in left occipital cortex and posterior Sylvian regions (all $t_{12} > 2$).

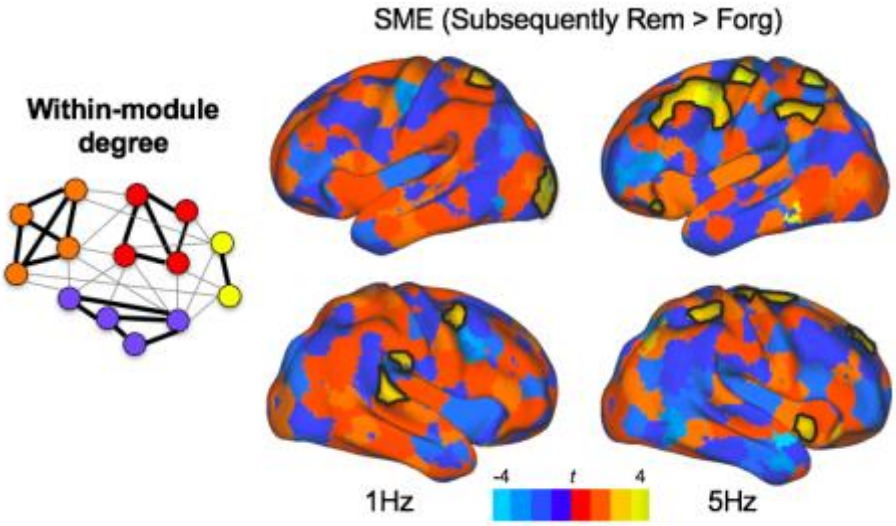

Figure 9. Within-Module Degree (WMD) associated with subsequent memory effects (SMEs) across rTMS conditions.

In sum, consistent with the compensation hypothesis, we found that the 1-Hz rTMS (1) reduced the SME univariate activity in LMFG and (2) increased WMD in left PFC, particularly between left PFC and contralateral right PFC regions, and that these two effects were connected to each other, as indicated by (3) a negative correlation between the reduction in LMFG activity (local dysfunction) and the increase in WMD increase (global over-recruitment). The fact that this last effect occurred for remembered but not for forgotten trials is also consistent with the compensation hypothesis. In contrast, a 5-Hz rTMS condition that enhanced local activity only led to an increase in local connectivity (WMD).

Linking rTMS-related changes on global connectivity to white-matter integrity

We found that global connectivity (BMD) of the stimulated LMFG region was enhanced by a 1-Hz rTMS condition that reduced local activity but not by a 1-Hz rTMS condition

that increased local activity. This finding is consistent with the compensation hypothesis that local dysfunction is counteracted by global over-recruitment. However, global over-recruitment depends on the integrity of white-matter tracts connecting distant brain regions. Thus, the effects of rTMS on functional connectivity should be correlated with white-matter integrity, particularly in the 1-Hz rTMS condition which is the one recruiting global connectivity. Thus, our second prediction was that *the global connectivity of the stimulated region should be correlated with white-matter integrity in the 1-Hz but not the 5-Hz rTMS condition.*

To test this second prediction, we quantified the relationships between white-matter integrity and the effects of 5-Hz and 1-Hz rTMS on memory-related functional connectivity for the stimulated LMFG region (xyz center of mass: -45, 18, 40, see **Figure 10A**). Pairwise t-tests revealed that the within-module connections, the correlation between white-matter integrity and functional connectivity was similarly correlated for 5-Hz and 1-Hz rTMS, whereas for between-module connections, white-matter integrity was much more strongly correlated with functional connectivity pattern for 1-Hz than for 5-Hz rTMS ($t_{13} = 2.76$, $p < 0.01$, see **Figure 10B**). Outside left PFC, we did not find any significant difference between 1-Hz and 5-Hz rTMS on structure-function relationships. In sum, consistent with our second prediction,

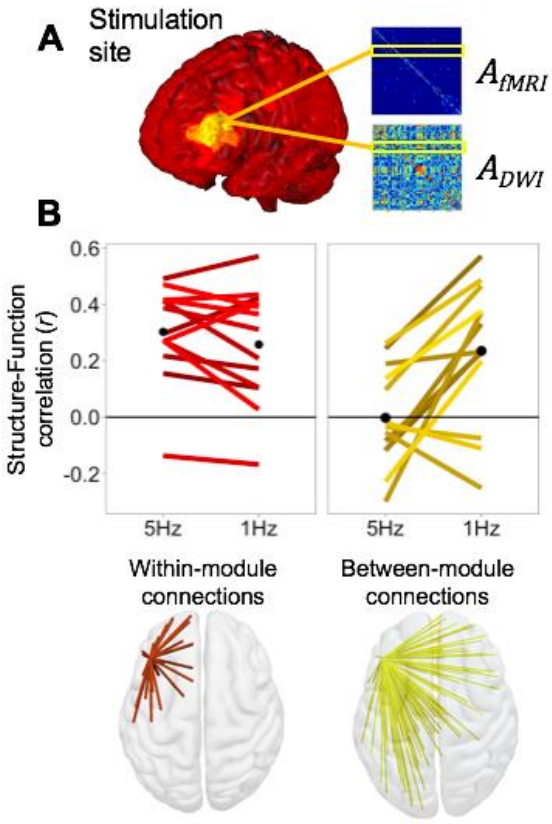

Figure 10. Structure-function relationships as a function of rTMS frequency and connection type. We represent the evolution of the correlation quality between structural and functional connectivity from a localized stimulation site (**A**) either *within* a local community, or *between* distinct modular communities. (**B**) Pairwise comparisons reveal consistently strong structure-function associations for network connections within the local module. In contrast, when considering between-module connections, this relationship was stronger for 1Hz than 5Hz memory networks, suggesting a the above increase in BMD connectivity associated with 1Hz rTMS is constrained by white matter connectivity.

Discussion

Our overarching goal was to investigate the neural mechanisms linking local and global TMS effects by combining rTMS with fMRI and DTI. The study yielded two main findings. *First, a reduction in local activity was associated with an increase global connectivity.* Consistent with the compensation hypothesis, the 1-Hz rTMS condition that caused

under-activation at the stimulation site, led to an increase in global connectivity (BMD). In contrast, the 5-Hz rTMS condition that caused over-activation at the stimulation site yielded only an increase in local connectivity (WMD). *Second, the increase in global connectivity was modulated by white-matter integrity.* In keeping with the idea that functional connectivity is constrained by white-matter integrity, in the 1-Hz rTMS, but not 5-Hz rTMS condition, global connectivity of the stimulated region was correlated white-matter integrity. The sections below discuss these two findings and then consider their relations with aging.

A reduction in local activity was associated with an increase global connectivity

A critical finding from the current analysis is that 5Hz stimulation to a memory-specific target was associated with greater within-module connectivity (WMD), while 1Hz rTMS engendered a more distributed pattern of connectivity with other modules (BMD). When examining the subject-wise relationship between univariate activity and BMD connectivity, we found a strong negative relationship for successfully remembered but not forgotten trials specific to the 1Hz condition, evidencing an adaptive relationship between local suppression of activity and more distant connectivity (**Figs. 5, 6**). This result suggests a highly responsive global network that is able to shift connectivity patterns in response to the depletion of local resources by relying on a more distributed pattern of connectivity.

The dynamic relationship between local and distant connectivity has begun to have been explored in a systematic way through the use of the graph-theoretic concept of “communities” or modules. A number of recent analyses have demonstrated that both weak intramodular connections and more distant, intermodular connections play a crucial role in establishing modular structure and predictive cognitive outcomes (Gallos

et al., 2012; Santarnecchi et al., 2014). In these frameworks, as in our own, local interactions within a module characterize specialized functions (Sporns and Betzel, 2016), a trend that appears to develop through adolescence and across the lifespan (Power et al., 2010; Geerligs et al., 2015). Furthermore, the relationship between modularity and cognitive performance is typically positive, especially when the cognitive demands of the task can be localized to a discrete, localized processing system (e.g., working memory, as in Stevens et al., 2012) or when behaviors become more specialized over the lifespan (e.g., syntax, as in Meunier et al., 2014). Conversely, task operations which require greater global communication (and therefore reductions in functional modularity) are typically associated with cognitions requiring integration from multiple cortical communities, including visual awareness (Godwin et al., 2015) or episodic memory formation (Geib et al., 2015), consistent with global workspace models of brain function (Dehaene et al., 2011).

In the current study we used static community boundaries to demonstrate how different stimulation conditions affect task-related memory processing within and across those boundaries. We showed that stimulation-induced reductions in local activity after 1Hz rTMS resulted in increased connectivity between left PFC and other ipsilateral and contralateral modules in prefrontal and parietal regions, suggesting a frequency-specific role for this type of network reorganization. As noted above, frequency-specific TMS can selectively alter intrinsic neural dynamics between and within functionally specialized large-scale brain modules. This hypothesis is supported by the results of empirical and simulation studies, which suggest that the functional effects of focal changes in neural activity may extend outside a functionally segregated network (Bestmann et al., 2004; Alstott et al., 2009; van Dellen et al., 2013). Because large-scale modules are positioned

at an intermediate scale between local and global integration, they may play a critical role in integrating local changes without reorganizing the backbone of large-scale brain communication.

The increase in global connectivity was modulated by white-matter integrity

Turning to our cross-modal network analysis, we found that the structural networks given by diffusion-weighted tractography reliably constrained the functional connectivity. We found that while within-module connectivity correlates with functional networks derived from both the post-5Hz and post-1Hz rTMS fMRI, the more distant between-module connectivity more strongly predicted 1Hz than 5Hz success networks. This pattern of results mirrors our earlier WMD/BMD findings, suggesting that global, between-module connectivity patterns are constrained by structural connectivity. While regional correlations between diffusion based structural connectivity and task-based functional connectivity remained consistently above chance—reflecting a general trend than structural connectivity may help explain some, but not all of the variance in functional connectivity (Honey et al., 2009; Betzel et al., 2014)—this relationship was most pronounced in the connections emanating from the stimulation site.

The finding that long-range connectivity (BMD) was correlated with white-matter integrity offers a mechanistic explanation for the anatomical basis for localizing the effects of changes at a proximal site at more distant locations in the aging brain, and suggests that will take advantage of existing structural architecture (Daselaar et al., 2014). However, recent longitudinal studies of structural-function relationships have shown a very selective topological pattern of pathways showing this effect (Fjell et al., 2016), a finding that is unsurprising when considering 1) the heterogeneity of regional connectivity, the sparsity of structural networks (~80%, depending on the parcellation

scheme (Wang et al., 2015), and 3) differences in reported age-trajectories for microstructural WM tract properties and FC (Walhovd et al., 2011; Bartzokis et al., 2012). Therefore, there is sufficient evidence to suggest that these function-structure relationships are best characterized only by specific fiber systems during specific conditions. Such multimodal relationships may not emerge when the functional networks are at rest, but only during active cognitive operations when those structural connections are necessary to the cognition at hand. In the context of our finding, such flexibility is in keeping with the expensive nature of long-range connections, as well as the dynamic nature of regional brain interactions.

Beyond increasing the ability to use combined brain imaging and stimulation to investigate brain function in normative populations, the present results suggest that DTI-based TMS targeting can extend the effectiveness of TMS in therapeutic applications. One obstacle for using TMS for effective treatments in memory disorders is that the brain region most critical for memory and most affected, the hippocampus, sits deep inside the brain, beyond the reach of direct TMS effects. The current finding suggests that cortical stimulation propagates to distant cortical and subcortical sites in a manner predicted by the 1st-order structural connectivity of the stimulation site. However, it remains unclear how such relationships observed may be affected by more large-scale system dynamics. Future work focused on the stability and changeability of network connectivity in memory states in the aging brain may therefore provide new information on the effectiveness of brain stimulation technologies as a therapeutic measure for cognitive decline.

Both findings have implications for aging research

The finding that a reduction in local activity was associated with an increase in global connectivity is consistent the functional neuroimaging evidence that older adults, who show deficits in specific brain regions such as PFC, tend to display a more widespread pattern of brain activity than younger adults (Spaniol et al., 2009; Spreng et al., 2010). This effect is often attributed to compensatory mechanisms (Reuter-Lorenz and Park, 2014), which could also explain the current rTMS findings. While typical assessments of these patterns are made across cohorts of younger and older adults, the current results represent a novel means of probing aging brain function by using a frequency-specific changes in cognitive and network state. The impact of TMS on neural functioning in aging populations during memory tasks is still in its infancy. Nonetheless, new consensus is building towards the specific stimulation parameters that engender a positive effect on cognitive function in physiological and pathological aging (for review, see Hsu et al., 2015), and a number of studies have elicited a positive role for TMS-induced excitability, largely utilizing excitatory 5-10Hz trains of rTMS (Luber et al., 2007; Eliasova et al., 2014; Brambilla et al., 2015).

Increased functional connectivity in healthy aged populations or in risk groups such as Alzheimer disease patients is often interpreted as a compensatory response to declining brain health (Agosta et al., 2012; Sheline and Raichle, 2013; Gomez-Ramirez et al., 2015), despite the fact that these increases are observed during resting state scans. Similarly, age-related examinations of graph-theoretic measures has typically relied on resting brain activity, and generally describe a decline in the network cohesion (i.e., modularity) when compared with younger counterparts (Betzel et al., 2014; Cao et al., 2014). The utility of this task-free approach is limited. Growing evidence in task-

related studies of whole-brain connectivity suggests that, despite this reduction in functional specificity, older adults are able to adapt the functional connectivity between functional networks (or modules) in order to adapt to task demands (Geerligs et al., 2014; Meunier et al., 2014).

A critical component of characterizing a neural response as compensatory relies on the nature of its relationship to successful cognition. Our dependent measure of global integration, BMD, selectively increased during successfully remembered trials when local processing was disrupted by 1Hz rTMS. The cognitive relevance of this result is supported by the result that BMD at the stimulation site during concurrent stimulation during a task-free rest period was *unrelated* to the above increase in BMD for successfully remembered than forgotten trials (**Figure 8**). This result helps us reject the hypothesis that increases in contralateral connectivity are explained by an age-related lack of inhibition of the contralateral hemisphere (Colcombe et al., 2005), a model of interhemispheric interactions which explains coordinated motor functioning (Langan et al., 2010; Fling et al., 2011), but does not appear to transpose to prefrontal interactions (Davis et al., 2012; Brambilla et al., 2015). Moreover, univariate activity and functional connectivity demonstrates stimulation- and topologically-selective relationship (**Figure 7**), such that a negative relationship was observed between these factors after 1Hz rTMS. This finding helps to build a bridge between two neural levels of explanation, and suggests a precise mechanism by which more generalized age-related phenomena such as compensation may operate within specific individuals.

Conclusions

The current analysis provides novel evidence that aging brains utilizes a flexible set of neural dynamics to accomplish the same cognitive task under different stimulation conditions. Whereas 5-Hz rTMS increased memory-related local connectivity (WMD), the application of 1Hz rTMS engendered more global connectivity (BMD) to different brain modules located bilaterally from the site of stimulation. These more global effects were strongly constrained by structural connectivity derived from diffusion-weighted tractography. These results provide an integrated, causal explanation of the network interactions associated with successful memory encoding in older adults.

References

Agosta F, Pievani M, Geroldi C, Copetti M, Frisoni GB, Filippi M (2012) Resting state fMRI in Alzheimer's disease: beyond the default mode network. Neurobiology of aging 33:1564-1578.

Alstott J, Breakspear M, Hagmann P, Cammoun L, Sporns O (2009) Modeling the impact of lesions in the human brain. PLoS computational biology 5:e1000408.

Bartzokis G, Lu PH, Heydari P, Couvrette A, Lee GJ, Kalashyan G, Freeman F, Grinstead JW, Villablanca P, Finn JP, Mintz J, Alger JR, Altshuler LL (2012) Multimodal magnetic resonance imaging assessment of white matter aging trajectories over the lifespan of healthy individuals. Biol Psychiatry 72:1026-1034.

Bellec P, Benhajali Y, Carbonell F, Dansereau C, Albouy G, Pelland M, Craddock C, Collignon O, Doyon J, Stip E, Orban P (2015) Impact of the resolution of brain parcels on connectome-wide association studies in fMRI. NeuroImage.

Bestmann S, Baudewig J, Siebner HR, Rothwell JC, Frahm J (2004) Functional MRI of the immediate impact of transcranial magnetic stimulation on cortical and subcortical motor circuits. Eur J Neurosci 19:1950-1962.

Betzel RF, Byrge L, He Y, Goni J, Zuo XN, Sporns O (2014) Changes in structural and functional connectivity among resting-state networks across the human lifespan. Neuroimage 102 Pt 2:345-357.

Brambilla M, Manenti R, Ferrari C, Cotelli M (2015) Better together: Left and right hemisphere engagement to reduce age-related memory loss. Behav Brain Res 293:125-133.

Cabeza R (2002) Hemispheric asymmetry reduction in older adults: the HAROLD model. Psychol Aging 17:85-100.

Cao M, Wang JH, Dai ZJ, Cao XY, Jiang LL, Fan FM, Song XW, Xia MR, Shu N, Dong Q, Milham MP, Castellanos FX, Zuo XN, He Y (2014) Topological organization of the human brain functional connectome across the lifespan. Dev Cogn Neurosci 7:76-93.

Chang YT, Leahy RM, Pantazis D (2012) Modularity-based graph partitioning using conditional expected models. Phys Rev E Stat Nonlin Soft Matter Phys 85:016109.

Chang YT, Pantazis D, Leahy RM (2014) To cut or not to cut? Assessing the modular structure of brain networks. NeuroImage 91:99-108.

Clapp WC, Rubens MT, Gazzaley A (2010) Mechanisms of working memory disruption by external interference. Cereb Cortex 20:859-872.

Colcombe SJ, Kramer AF, Erickson KI, Scalf P (2005) The implications of cortical recruitment and brain morphology for individual differences in inhibitory function in aging humans. Psychol Aging 20:363-375.

Daselaar SM, Iyengar V, Davis SW, Eklund K, Hayes SM, R. C (2014) Less wiring, more firing: Low-performing older adults compensate for impaired

white matter with greater neural activity. . Cerebral Cortex (available online).

Davis SW, Kragel JE, Madden DJ, Cabeza R (2012) The architecture of cross-hemispheric communication in the aging brain: linking behavior to functional and structural connectivity. Cereb Cortex 22:232-242.

de Vries PM, de Jong BM, Bohning DE, Hinson VK, George MS, Leenders KL (2012) Reduced parietal activation in cervical dystonia after parietal TMS interleaved with fMRI. Clin Neurol Neurosurg 114:914-921.

Dehaene S, Changeux JP, Naccache L (2011) The Global Neuronal Workspace Model of Conscious Access: From Neuronal Architectures to Clinical Applications. Res Per Neurosci:55-84.

Dennis NA, Hayes SM, Prince SE, Madden DJ, Huettel SA, Cabeza R (2008) Effects of aging on the neural correlates of successful item and source memory encoding. J Exp Psychol Learn Mem Cogn 34:791-808.

Eliasova I, Anderkova L, Marecek R, Rektorova I (2014) Non-invasive brain stimulation of the right inferior frontal gyrus may improve attention in early Alzheimer's disease: a pilot study. J Neurol Sci 346:318-322.

Feredoes E, Heinen K, Weiskopf N, Ruff C, Driver J (2011) Causal evidence for frontal involvement in memory target maintenance by posterior brain areas during distracter interference of visual working memory. Proceedings of the National Academy of Sciences of the United States of America 108:17510-17515.

Fjell AM, Sneve MH, Grydeland H, Storsve AB, Amlien IK, Yendiki A, Walhovd KB (2016) Relationship between structural and functional connectivity change across the adult lifespan: A longitudinal investigation. Hum Brain Mapp.

Fling BW, Walsh CM, Bangert AS, Reuter-Lorenz PA, Welsh RC, Seidler RD (2011) Differential callosal contributions to bimanual control in young and older adults. Journal of cognitive neuroscience 23:2171-2185.

Fornito A, Zalesky A, Breakspear M (2015) The connectomics of brain disorders. Nat Rev Neurosci 16:159-172.

Fornito A, Harrison BJ, Zalesky A, Simons JS (2012) Competitive and cooperative dynamics of large-scale brain functional networks supporting recollection. Proc Natl Acad Sci U S A 109:12788-12793.

Fornito A, Yoon J, Zalesky A, Bullmore ET, Carter CS (2011) General and specific functional connectivity disturbances in first-episode schizophrenia during cognitive control performance. Biol Psychiatry 70:64-72.

Gallos LK, Makse HA, Sigman M (2012) A small world of weak ties provides optimal global integration of self-similar modules in functional brain networks. Proc Natl Acad Sci U S A 109:2825-2830.

Garyfallidis E, Brett M, Correia MM, Williams GB, Nimmo-Smith I (2012) QuickBundles, a Method for Tractography Simplification. Frontiers in neuroscience 6:175.

Garyfallidis E, Brett M, Amirbekian B, Rokem A, van der Walt S, Descoteaux M, Nimmo-Smith I, Dipy C (2014) Dipy, a library for the analysis of diffusion MRI data. Frontiers in neuroinformatics 8:8.

Geerligs L, Maurits NM, Renken RJ, Lorist MM (2014) Reduced specificity of functional connectivity in the aging brain during task performance. Hum Brain Mapp 35:319-330.

Geerligs L, Renken RJ, Saliasi E, Maurits NM, Lorist MM (2015) A Brain-Wide Study of Age-Related Changes in Functional Connectivity. Cereb Cortex 25:1987-1999.

Geib BR, Stanley ML, Wing EA, Laurienti PJ, Cabeza R (2015) Hippocampal Contributions to the Large-Scale Episodic Memory Network Predict Vivid Visual Memories. Cereb Cortex.

Godwin D, Barry RL, Marois R (2015) Breakdown of the brain's functional network modularity with awareness. Proc Natl Acad Sci U S A 112:3799-3804.

Gomez-Ramirez J, Li Y, Wu Q, Wu J (2015) A Quantitative Study of Network Robustness in Resting-State fMRI in Young and Elder Adults. Front Aging Neurosci 7:256.

Gong G, He Y, Concha L, Lebel C, Gross DW, Evans AC, Beaulieu C (2009) Mapping anatomical connectivity patterns of human cerebral cortex using in vivo diffusion tensor imaging tractography. Cereb Cortex 19:524-536.

Guimera R, Nunes Amaral LA (2005) Functional cartography of complex metabolic networks. Nature 433:895-900.

Hanslmayr S, Matuschek J, Fellner MC (2014) Entrainment of prefrontal beta oscillations induces an endogenous echo and impairs memory formation. Curr Biol 24:904-909.

Honey CJ, Sporns O, Cammoun L, Gigandet X, Thiran JP, Meuli R, Hagmann P (2009) Predicting human resting-state functional connectivity from structural connectivity. Proc Natl Acad Sci U S A 106:2035-2040.

Hoogendam JM, Ramakers GM, Di Lazzaro V (2010) Physiology of repetitive transcranial magnetic stimulation of the human brain. Brain stimulation 3:95-118.

Horn A, Ostwald D, Reisert M, Blankenburg F (2014) The structural-functional connectome and the default mode network of the human brain. Neuroimage 102 Pt 1:142-151.

Hsu WY, Ku Y, Zanto TP, Gazzaley A (2015) Effects of noninvasive brain stimulation on cognitive function in healthy aging and Alzheimer's disease: a systematic review and meta-analysis. Neurobiology of aging 36:2348-2359.

Langan J, Peltier SJ, Bo J, Fling BW, Welsh RC, Seidler RD (2010) Functional implications of age differences in motor system connectivity. Front Syst Neurosci 4:17.

Luber B, Lisanby SH (2014) Enhancement of human cognitive performance using transcranial magnetic stimulation (TMS). Neuroimage 85 Pt 3:961-970.

Luber B, Kinnunen LH, Rakitin BC, Ellsasser R, Stern Y, Lisanby SH (2007) Facilitation of performance in a working memory task with rTMS stimulation of the precuneus: frequency- and time-dependent effects. Brain Res 1128:120-129.

Meunier D, Stamatakis EA, Tyler LK (2014) Age-related functional reorganization, structural changes, and preserved cognition. Neurobiology of aging 35:42-54.

Nahas Z, Lomarev M, Roberts DR, Shastri A, Lorberbaum JP, Teneback C, McConnell K, Vincent DJ, Li X, George MS, Bohning DE (2001) Unilateral left prefrontal transcranial magnetic stimulation (TMS) produces intensity-dependent bilateral effects as measured by interleaved BOLD fMRI. Biol Psychiatry 50:712-720.

Newman ME (2006) Modularity and community structure in networks. Proc Natl Acad Sci U S A 103:8577-8582.

Paller KA, Wagner AD (2002) Observing the transformation of experience into memory. Trends Cogn Sci 6:93-102.

Power JD, Fair DA, Schlaggar BL, Petersen SE (2010) The development of human functional brain networks. Neuron 67:735-748.

Reuter-Lorenz PA, Park DC (2014) How does it STAC up? Revisiting the scaffolding theory of aging and cognition. Neuropsychol Rev 24:355-370.

Santarnecchi E, Galli G, Polizzotto NR, Rossi A, Rossi S (2014) Efficiency of weak brain connections support general cognitive functioning. Hum Brain Mapp 35:4566-4582.

Saur D, Ronneberger O, Kummerer D, Mader I, Weiller C, Kloppel S (2010) Early functional magnetic resonance imaging activations predict language outcome after stroke. Brain 133:1252-1264.

Schneider SA, Pleger B, Draganski B, Cordivari C, Rothwell JC, Bhatia KP, Dolan RJ (2010) Modulatory effects of 5Hz rTMS over the primary somatosensory cortex in focal dystonia--an fMRI-TMS study. Mov Disord 25:76-83.

Seeley WW, Crawford RK, Zhou J, Miller BL, Greicius MD (2009) Neurodegenerative diseases target large-scale human brain networks. Neuron 62:42-52.

Sheline YI, Raichle ME (2013) Resting state functional connectivity in preclinical Alzheimer's disease. Biol Psychiatry 74:340-347.

Smith SM, Jenkinson M, Johansen-Berg H, Rueckert D, Nichols TE, Mackay CE, Watkins KE, Ciccarelli O, Cader MZ, Matthews PM, Behrens TE (2006) Tract-based spatial statistics: voxelwise analysis of multi-subject diffusion data. Neuroimage 31:1487-1505.

Spaniol J, Grady C (2012) Aging and the neural correlates of source memory: over-recruitment and functional reorganization. Neurobiology of aging 33:425 e423-418.

Spaniol J, Davidson PS, Kim AS, Han H, Moscovitch M, Grady CL (2009) Event-related fMRI studies of episodic encoding and retrieval: meta-analyses using activation likelihood estimation. Neuropsychologia 47:1765-1779.

Sporns O, Betzel RF (2016) Modular Brain Networks. Annu Rev Psychol 67:613-640.

Spreng RN, Wojtowicz M, Grady CL (2010) Reliable differences in brain activity between young and old adults: a quantitative meta-analysis across multiple cognitive domains. Neurosci Biobehav Rev 34:1178-1194.

Stevens AA, Tappon SC, Garg A, Fair DA (2012) Functional brain network modularity captures inter- and intra-individual variation in working memory capacity. PloS one 7:e30468.

Tzourio-Mazoyer N, Landeau B, Papathanassiou D, Crivello F, Etard O, Delcroix N, Mazoyer B, Joliot M (2002) Automated anatomical labeling of activations in SPM using a macroscopic anatomical parcellation of the MNI MRI single-subject brain. Neuroimage 15:273-289.

van Dellen E, Hillebrand A, Douw L, Heimans JJ, Reijneveld JC, Stam CJ (2013) Local polymorphic delta activity in cortical lesions causes global decreases in functional connectivity. Neuroimage 83:524-532.

Walhovd KB, Westlye LT, Amlien I, Espeseth T, Reinvang I, Raz N, Agartz I, Salat DH, Greve DN, Fischl B, Dale AM, Fjell AM (2011) Consistent neuroanatomical age-related volume differences across multiple samples. Neurobiology of aging 32:916-932.

Wang JX, Rogers LM, Gross EZ, Ryals AJ, Dokucu ME, Brandstatt KL, Hermiller MS, Voss JL (2014) Targeted enhancement of cortical-hippocampal brain networks and associative memory. Science 345:1054-1057.

Wang Z, Dai Z, Gong G, Zhou C, He Y (2015) Understanding structural-functional relationships in the human brain: a large-scale network perspective. Neuroscientist 21:290-305.

Zemke AC, Heagerty PJ, Lee C, Cramer SC (2003) Motor cortex organization after stroke is related to side of stroke and level of recovery. Stroke 34:e23-28.

Zhong S, He Y, Gong G (2015) Convergence and divergence across construction methods for human brain white matter networks: an assessment based on individual differences. Human brain mapping 36:1995-2013.

Zimmermann J, Ritter P, Shen K, Rothmeier S, Schirner M, McIntosh AR (2016) Structural architecture supports functional organization in the human aging brain at a regionwise and network level. Hum Brain Mapp.